Relative Wavelet Energy as a diagnosis tool for PEM Fuel Cells

E. Pahon, D. Hissel, S. Jemei
Univ. Bourgogne Franche-Comte,
Univ. Franche-Comte,
FEMTO-ST UMR CNRS 6174,
FCLAB Research Federation FR CNRS 3539,
Rue Ernest Thierry Mieg, 90010 Belfort Cedex, France
{elodie.pahon, daniel.hissel, samir.jemei}@univ-fcomte.fr

N. Yousfi-Steiner
Univ. Bourgogne Franche-Comte,
Univ. Franche-Comte,
LABEX ACTION CNRS,
FEMTO-ST UMR CNRS 6174,
FCLAB Research Federation FR CNRS 3539,
Rue Ernest Thierry Mieg, 90010 Belfort Cedex, France
nadia.steiner@univ-fcomte.fr

***Abstract*— This paper deals with the relative wavelet energy as a diagnosis tool for PEMFC. The reliability and the durability of the fuel cell system have to be improved and the diagnosis approach is a way to extend the PEMFC lifetime. A signal-based method is used to estimate the state of health of the system. The energetic distribution is given according to different experimental conditions. The energy contents of a voltage signal are selected and analyzed to define the PEMFC's state of health. A clustering step is added to identify a fault. This study is based on a high air stoichiometry fault.**

Keywords—Diagnosis; PEMFC; Relative wavelet energy, Clustering, Signal-based method.

I. INTRODUCTION

As fuel cell seems to be a promise alternative to fossil fuel, this technology is more and more studied, developed and used in vehicle applications [1-3]. A limit of this electrochemical device is the lifetime [4]. To solve this problem, some diagnosis methodologies are developed in order to prevent irreversible damages of the fuel cell system.

A mathematical tool called wavelet transform is used in several domains and for different aims. The wavelet analysis is exploited for the energy management of electrical and hybrid vehicles as in [5]. In [6], authors propose a comparative study of energy management schemes for a fuel cell hybrid emergency power system of more electric aircraft. Various sources are stored on-board as: fuel cell, lithium-ion batteries, supercapacitors, DC/DC and AC/DC converters. The solicitations of each device which impact their lifetime are measured by using wavelet analysis. The main comparisons concern the hydrogen consumption, the state-of-charge of the batteries and supercapacitors and the efficiency. Two energy management are studied in [7]. The wavelet transform approach is used to forecast the power demand of batteries and supercapacitors to distribute the energy depending on the different sources on-board the hybrid electrical vehicle.

In [8], a specific aspect of the wavelet analysis named wavelet packet transform is used to diagnose a flooding state inside a PEMFC, thanks to the stack voltage measurement. The signal-based approach can be adapted to a large set of fuel cell configurations and applications as in [9] where the method helps diagnosing a SOFC system working in various operating conditions.

In medicine, the wavelet transform (WT) is widely used for processing all kind of signals as: electrocardiogram (ECG), electroencephalogram (EEG) and electromyogram (EMG) signals. In [10], the wavelet transform allows denoising the ECG signals by filtering successively the initial signal measured. Thanks to this approach, the diagnosis results are easier to get. The wavelet transform approach has also been used for ECG signals' classification, by post-processing the wavelet coefficients obtained after decomposing of the dedicated signal [11]. The detector in [12] proposes an algorithm to help detect seizures in long-term invasive-EEG based on low computational methods such as power spectral density and wavelet analysis. The detector in [12] has been tested on 21 invasive invasive-EEG records, and a sensitivity of 85.39% was achieved. In [13], Akar et al. decomposed the cardiovascular activity by using wavelet packet analysis in order to treat the major depression patients. Accumulative clinical proof recommends that dysfunction in autonomic nervous system activity has a significant role in depression [14-15]. Niegowski et al. present a novel approach aimed at removing ECG perturbation from single-channel surface EMG recordings by means of unsupervised learning of wavelet-based intensity images. The general idea is to combine the suitability of certain wavelet decomposition bases which provide sparse electrocardiogram time-frequency representations, with the capacity of non-negative matrix factorization for extracting patterns from images which ensures proper signal decomposition in a wide range of ECG [16].

One of the characteristic values calculated from the wavelets coefficients is the relative wavelet energy (RWE). This parameter is used by some authors for electroencephalogram signals processing [17]. The RWE gives some information about the similarity between two signals [18-19].

978-1-5090-3528-1/16/$31.00 ©2016 IEEE

In this paper, a similar methodology is applied to a PEMFC for fault diagnosis in order to extend the lifetime for vehicle applications.

The aim is to discriminate two states-of-health (SoH), namely: "normal" operation and a faulty operation induced by a "high air stoichiometry". This fault can appear in a failure compressor case. The air flow supplies by the compressor is not convenient for the fuel cell system and cause some degradations and damages on the fuel cell if this state-of-health is not detecting on-time.

The stack voltage is the input signal used to provide diagnosis results. Hence, the developed signal-based method is non-intrusive and low cost as the existing voltage sensor in the system is used also for diagnosis purposes.

II. DIAGNOSIS PRINCIPLE

Figure 1 represents the different steps of the diagnosis methodology applied to the stack voltage signal in this work, namely: voltage monitoring, Wavelet transform, feature extraction (RWE) and classification. Different voltage signals are acquired during a "high air stoichiometry" fault. Experimentally, the air stoichiometry is increased on the test bench from the nominal value 2 to the maximal acceptable value 5.

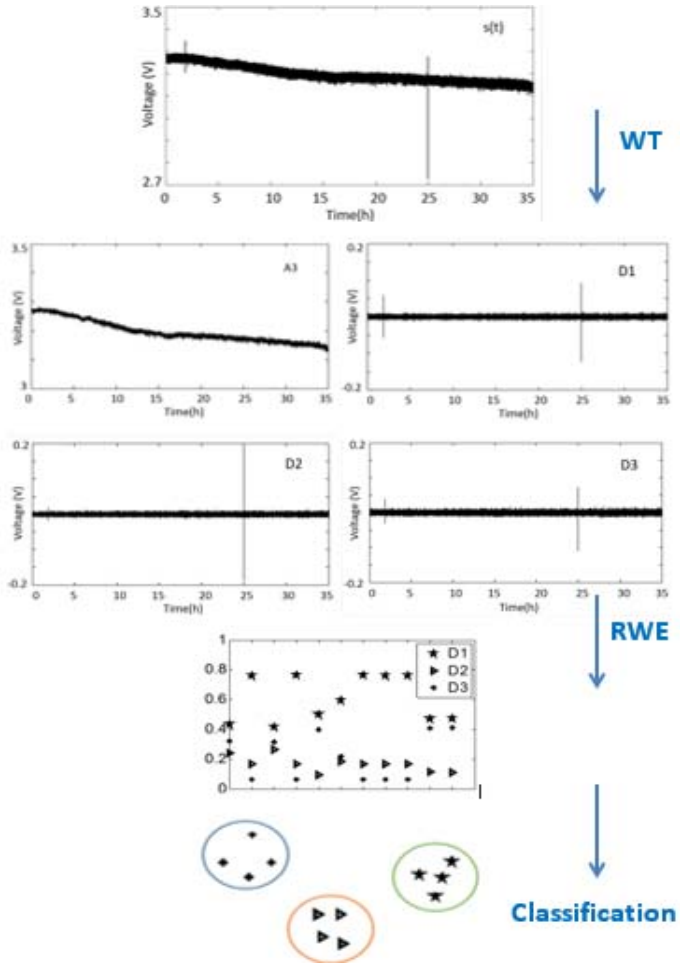

Fig. 1. Principle of the signal-based fault diagnosis method

The WT is then applied. The initial signal *s(t)* is split into approximation and detail signals. According to a suitable decomposition level *j* and wavelet ψ, *j* approximation signals and *j* details signals are obtained (see Fig. 2).

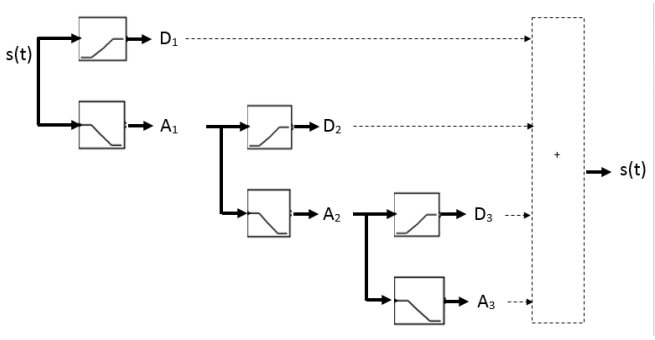

Fig. 2. Decomposition and recomposition of a signal *s(t)* thanks to WT

In this work, a specific Daubechies wavelet (*db4*) with 5 decomposition levels [20] is used as: this kind of wavelet is widely used in the literature for diagnosis task and 5 decomposition level are sufficient to study the behavior of the fuel cell because it is within its frequency.

The wavelet decomposition analysis allows seeing the behavior of the fuel cell for different frequency bands thanks to the scaling factor. Thus, for an acquired signal it is possible to evaluate the behavior of the fuel cell for multiple frequencies linked to the decomposition level.

In this case, that corresponds to frequency band comprised between 1Hz (the acquisition frequency) and 0.031Hz (the minimal frequency of the last detail signal D_5).

A. FEATURE EXTRACTION

The feature extraction step consists of determining the energy contents of input stack voltage.

A voltage signal *s(t)* is collected for each variations of the air stoichiometry. As shown on figure 1, the wavelet transform (WT) is the first step, after voltage monitoring. A focus is done on the energy contents of the signal *s(t)* and especially on the energy contained in each detail ($D_1,\ldots,D_5$).

For each detail D_j of the wavelet decomposition, the energy E_j is calculated thanks to (2).

$$E_j = \sum_{j=1} |D_j(k)|^2 \quad (2)$$

where *j* is the level of decomposition.

The total energy of the signal is calculated by (3).

$$E_{tot} = \sum_j \sum_k |D_j(k)|^2 = \sum_j E_j \quad (3)$$

The RWE is the ratio between the energy of a detail and the total energy of the signal.

$$RWE = \frac{E_j}{E_{tot}} \quad (4)$$

B. SIGNAL CLASSIFICATION

The distribution of the energies contained in each detail signals, for a given operating condition is called energetic distribution. It allows showing some significant behaviors of the energy, for each detail signal, in order to estimate the SoH of the PEMFC. The approach would be to gather each same detail *Dj* without taking into account the operating conditions. Each detail D_j corresponds to a point inside the created scatterplot. If points are visually separable from others, a classification can be performed. The aim is to see if the energy of a detail D_j is separable from another energy of a detail D_j when the operating conditions are healthy or faulty and validate it. The Euclidean distance between the different groups can be calculated, to ensure that the classes are well separated.

III. EXPERIMENTAL APPLICATION

A. FUEL CELL

The data used are collected from the characterization of a 40-cell stack. Table 1 gives some characteristics of the investigated PEMFC.

TABLE I. TECHNICAL SPECIFICATIONS OF THE INVESTIGATED FUEL CELL

Number of cells	40
Cell area (cm²)	220
Nominal current density (A/cm²)	0.5
Nominal power (W)	3 080
Nominal reactant stoichiometry ratios (anode/cathode)	1.5/2
Cathode stoichiometry ratio	[1.5 : 5]
Nominal temperature (°C)	80
Nominal pressure (bar abs.)	1.5

B. TEST BENCH

The experimental tests are carried out on a 10kW test bench, allowing the maximal values of the PEMFC stack operating conditions. Several measurements are possible including the electric, fluidic and thermal parts. All these parameters are acquired thanks to a National Instruments acquisition system and controlled via a Labview graphical interface. The high air stoichiometry fault is managed from the software by increasing it.

C. HIGH AIR STOICHIOMETRY FAULT

When the air stoichiometry increases, the membrane is drying [21]. The air flow is more important, thus the water created by the electrochemical reaction is evacuate from the fuel cell more rapidly. This phenomena is reversible if the exposition time of drying is not too long and if the membrane is correctly humidified rapidly too. The severity of the drying fault depends on the membrane thickness [22-25]. In [26], the oxygen excess is regulated by an adjustable PID controller to make the fault reversible.

On a fuel cell system, this kind of fault is considered as frequent [27]. It can appear further to an air compressor failure or further an air flow control failure.

In our case, the high air stoichiometry is simulated on a test bench by changing and forcing the air stoichiometry value to a high one.

D. TEST PROTOCOL

The fault is tested several times to acquire a large amount of data for the diagnosis approach. The test protocol consists of starting the experiment at the nominal and healthy operating conditions. This is a necessary step before putting the fuel cell system in a faulty mode. This stage allows establishing the reference sample (healthy and nominal conditions) from which a "faulty" state can be defined and compared. The test protocol consists in increasing the magnitude of the fault and so, to be more and more harmful for the system.

The recommendations of the manufacturer give minimal and maximal admissible stoichiometry values. At the cathode side, it is possible to increase the stoichiometry value from 2 (nominal) to 5 (maximum).

Thus, different experimental measurement are done on the 40-cell stack as show on Fig. 3.

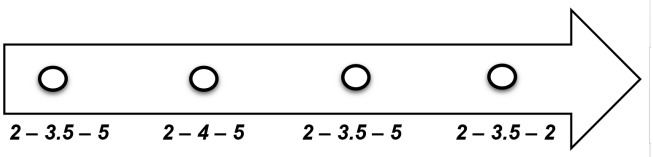

Fig. 3. Experimental variations of the high air stoichiometry

Four test protocols are exposed by taking into account different air stoichiometry increasing. For each, the experiment starts with the nominal air stoichiometry value: 2. After that, the air flow increases until reaches the maximal value:5.

Fig. 4 represents the evolution of the air stoichiometry depending on the time for one acquisition case.

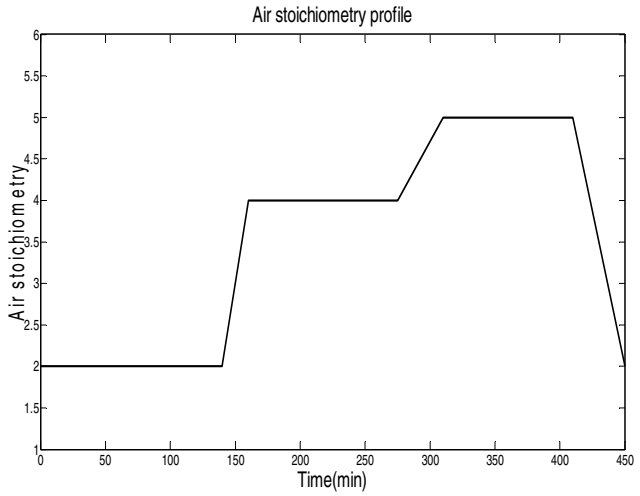

Fig. 4: Example of a high air stoichiometry profile

IV. RESULTS

The RWE is calculated with (4) for all the details coming from the stack voltage signals. For all the experiment series, 5 symbols representing details are given. Fig. 5 presents the results.

It is important to notice that in the nominal value of stoichiometry the detail D_1 has the highest energy value and its energy becomes very low when the cathode stoichiometry increases towards its maximal value. On the contrary, the energy of the detail D_5 is low on the nominal conditions and increases during the high air stoichiometry fault.

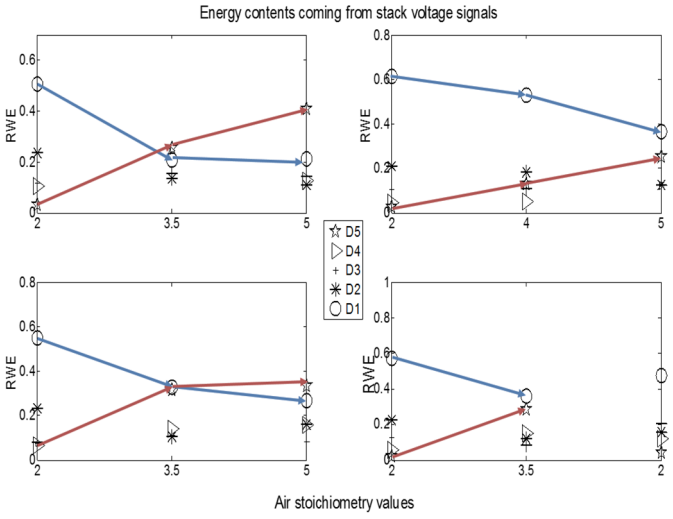

Fig. 5. RWE based on the stack voltage.

The *db4* wavelet conserved the energy. When the fuel cell operates under nominal conditions, the RWE of D_1 is low. It means that the signal D_1 is similar to the healthy input signal. When the air stoichiometry increases, the energy of D_5 increases too. The signal D_5 is similar to the faulty input voltage signal. Each detail signal belongs to a specific frequency band. For D_5 the frequencies are comprised between [0.016 ; 0.031] Hz. In [28], Wang et al. considered that in this frequency band where a high air stoichiometry fault could appear.

For the classification step, the two details D_1 and D_5 are observed. All extracted energies from D_1 and D_5 are plotted in the figure 6. Two point clouds are esthablished: one for D_1 and a second one for D_5.

For the first point cloud, two classes can be observed: one for a high air stoichiometry and a second for the nominal air stoichiometry. The remark is valid for the D_5 point cloud. The two point clouds are well separated in terms on energy as they belong to the one or the other category (FSC=2 or FSC>2).

Figure 6 gives the representation of the two groups into the two point clouds.

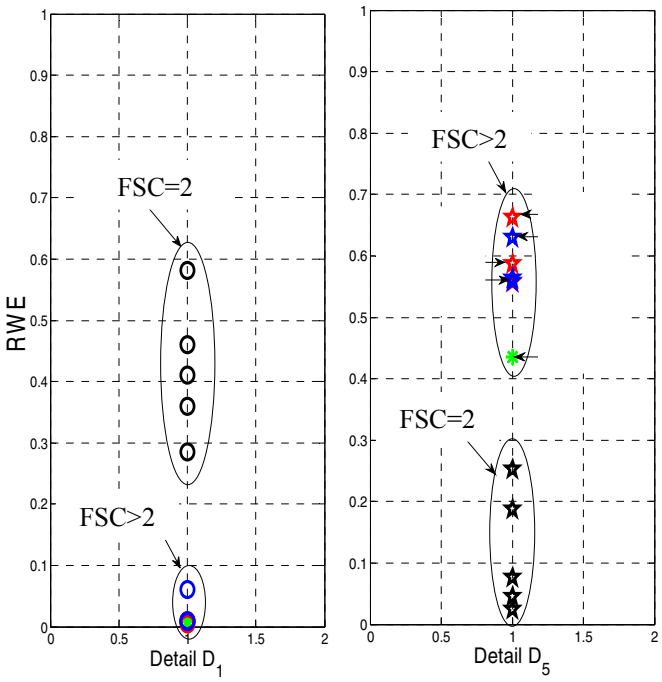

Fig. 6. D1 and D5 point clouds.

In order to validate this observation, the Euclidean distance between the two groups into the two point clouds can be calculated thanks to (5).

$$\mathrm{dist}(x,y) = \sqrt{\sum_{i=1}^{n}(x_i - y_i)^2} \qquad (5)$$

The first step is to define the centers of the two classes (FSC=2 and FSC>2) and to calculate the distance between them. The calculation is done a new time between the center of the group (FSC=2) and the different air stoichiometry values (FSC=3.5, FSC=4 and FSC=5). The aim is to know if

the Euclidean distance increasing between the group (FSC=2) and the different sub-groups by reaching the maximum stoichiometry value of 5. The table II presents the results.

TABLE II. DISTANCE BETWEEN TWO CLASSES

Considered classes	D_1	D_5
2 – 3.5	0.456	0.399
2 – 4	0.292	0.425
2 – 5	0.472	0.426

For D_1, the distance with the center of the nominal conditions group increases with the air stoichiometry. The more severe the fault is, the longer the distance between the two classes is. For D_5, the same behavior is observed. The two classes of the two point clouds are well separated and can be used for the PEMFC fault diagnosis.

For the high air stoichiometry fault, the fault diagnosis algorithm is able to detect variations of the air stoichiometry value. The detail signal representing the frequency band in which the fault appears, has a low relative energy. It means that the two compared signals are quite similar.

In addition, the point clouds is plotted for each level of severity of the fault and can reveal that the distance between the nominal class and the more severe fault class (FSC=2 – FSC=5) is higher than the distance between the nominal class and a less severe fault class (FSC=2 – FSC=3.5).

The classification step allows validating the identification phase of the diagnosis principle by giving an information of the magnitude of the fault encountered on the fuel cell system.

V. CONCLUSION

The developed algorithm allows detecting a state-of-health variations of PEM fuel cells. On the considered fault, several experiments are performed by increasing the air stoichiometry from the nominal value to the maximal admissible value. As soon as the air stoichiometry value changes, the energies contained in the detail signals change, that allows detecting a fault occurrence. The energy behavior evolves according to the successive increases of air stoichiometry. Two behavior distinguishes itself from others: for the detail D_1 and the detail D_5. The more severe the fault is, the highest the energy of the detail D_5 is, and conversely. According to the operating conditions, the energies of D_1 and D_5 seem to have a signature. It is confirmed by the data classification step. Two groups are clearly visible as the state-of-health is healthy (nominal operating conditions) or faulty (high air stoichiometry value). The wavelet analysis gives a first information concerning the fault occurrence by detecting a change in the energetic contents, then the tracking of the state-of-health with the RWE and the associated trend (especially balance between D1 and D5) allows estimating the severity of the fault that is finally validate by adding the classification step. This method confirms the magnitude of the fault estimated by the RWE trends and informs on the state-of-health by calculating distance between the group composed of healthy points and the faulty group regrouping all the other points in the energetic plan.

ACKNOWLEDGMENT

The authors acknowlege French ANR project DIAPASON2 and also the Labex ACTION, ANR-11-LABX-01-01, for financially supporting this work and offering the possibility of using their data.

REFERENCES

[1] J. Solano, D. Hissel, M.C. Péra. Energy management of an hybrid electric vehicle in degraded operation, 2014 IEEE Vehicle Power and Propulsion Conference (VPPC), 1-4.

[2] J.C. Olivier, G. Wasselynck, S. Chevalier, C. Josset, B. Auvity, G. Squadrito, D. Trichet, N. Bernard, S. Hmam. Multiphysics modelind and driving strategy optimization of an urban-concept vehicle, 2015 IEEE Vehicle Power and Propulsion Conference (VPPC), 1-6.

[3] A. Amamou, L. Boulon, S. Kelowani, K. Agbossou, P. Sicard. Thermal management strategies for cold start of automotive PEMFC, 2015 IEEE Vehicle Power and Propulsion Conference (VPPC), 1-6.

[4] F. Zenith, J. Tjonnas, I.J. Halvorsen. Control structure of a micro-combined heat and power fuel cell system for lifetime maximisation, 2014 IEEE Vehicle Power and Propulsion Conference (VPPC), 1-6.

[5] M. Ibrahim, S. Jemei, G. Wimmer, N. Yousfi-Steiner, C.C. Kokonendji, D. Hissel. Selection of mother wavelet and decomposition level for energy management in electrical vehicles including a fuel cell, Int. J. Hydrogen Energy, 2015, 1-11.

[6] S.N. Motapon, L.A. Dessaint, K. Al-Haddad. A comparative study of energy management schemes for a fuel cell hybrid emergency power system of more electric aircraft, IEEE Trans. On Ind. Electronics, 61, 3, 2013, 1320-1334.

[7] G. Livint, A.G. Stan. Control strategies for hybrid electric vehicles with two energy sources on board, Int. Conf. and Exposition on Electrical and Power Engineering 2014, 142-147.

[8] N. Yousfi-Steiner, D. Hissel, P. Moçotéguy, D. Candusso. Non intrusive diagnosis of polymer electrolyte fuel cells by wavelet packet transform, Int. J. Hydrogen Energy 36, 2011, 740-746.

[9] E. Pahon, N. Yousfi-Steiner, S. Jemei, D. Hissel, M.C. Péra, K. Wang, P. Mocçotéguy. Solid oxide fuel cell fault diagnosis and ageing estimation based on wavelet transform approach, Int. J. Hydrogen Energy 41, 31, 2016, 13678–13687.

[10] S. K. Yadav, R. Sinha, P. K. Bora, Electrocardiogram signal denoising using non-local wavelet transform domain filtering, Signal Processing, IET, 9, 1, 2015, 88-96.J. Clerk Maxwell, A Treatise on Electricity and Magnetism, 3rd ed., vol. 2. Oxford: Clarendon, 1892, pp.68-73.

[11] M. Nazarahari, S. G. Namin, A. H. D. Markazi, A. K. Anaraki. A multi-wavelet optimization approach using similarity measures for electrocardiogram signal classification, Biomedical Signal Processing and Control 20, 2015, 142-151.

[12] A. Correa, L. Orosco, P. Diez, E. Laciar. Automatic detection of epileptic seizure in longterm EEG records. Comput Biol Med 2015, 57, 66–73.

[13] S.A. Akar, S. Kara, V. Bilgiç. Investigation of heart rate variability in major depression patients using wavelet packet transform, Psychiatry Research, 238, 2016, 326 – 332.

[14] W. Agelink, C. Boz, H. Ullrich, J. Andrich. Relationship between major depression and heart rate variability: clinical consequences and implications for antidepressive treatment, PsychiatryRes 113, 2002, 139–149.

[15] J.C. Ehrenthal, C. Herrmann-Lingen, M. Fey, H. Schauenburg. Altered cardiovascular adaptability in depressed patients without heart disease, World J. Biol. Psychiatry 11, 2010, 586–593.

[16] M. Niegowski, M. Zivanovic. Wavelet-based unsupervised learning method for electrocardiogram suppression in surface electromyograms, Medical Engineering and Physics 38, 2016, 248-256.

[17] M. Salwani, Y. Jasmy, Relative wavelet energy as a tool to select suitable wavelet for artificial removal in EEG, First international conference on computer, communication and signal processing with special track on biomedical engineering, CCSP 2005, 282-287.

[18] O.A. Rosso, S. Blanco, J. Yordanova, V. Kolev, A. Figliola, M. Schurmann and E. Basar, Wavelet Entropy: A New Tool for Analysis of Short Duration Brain Electrical Signals, J. of Neuroscience Methods, 105, 2001, 65-75.

[19] O.A. Rosso, A. Figliola, Order/disorder in Brain Electrical Activity, Rev. Mex. Fis, 50, 2, 2004, 149-155.

[20] I. Daubechies. Ten lectures on wavelets, SIAM; 1992.

[21] A. Pozio, A. Cemmi, F. Mura, A. Masci, E. Serra, R.F. Silva. Long-term durability study of perfluoropolymer membranes in low humidification conditions, J. Solid State Electrochem., 15, 2011, 1209-1216.

[22] J.M. Le Canut, R.M. Abouatallah, D.A. Harrington. Detection of membrane brying, fuel cell flooding and anode catalyst poisoning on PEMFC stack by electrochemical impedance spectroscopy, J. Electrochem. Soc. 153, 2006, A857-A864.

[23] Y. Sone, P. Ekdunge, D. Simonsson. Proton conductivity of Nafion 117 as measured by a four-electrode AC impedance method, J. Electrochem. Soc. 143, 1996, 1254-1259.

[24] T.V. Nguyen, R.E. White. A water and heat management model for proton exchange membrane fuel cells, J. Electrochem. Soc. 140, 1993, 2178-2186.

[25] Y. Wang, C.Y. Wang. Dynamics of polymer electrolyte fuel cells undergoing load changes, Electrochemica Acta 51, 2006, 3924-3933.

[26] C. Lebreton, M. Benne, C. Damour, N. Yousfi-Steiner, B. Grondin-Perez, D. Hissel, J.P. Chabriat. Fault tolerant control strategy applied to PEMFC water management, Int. J. Hydrogen Energy, 40, 33, 2015, 10636-10646.

[27] S. Qu, X. Li, M. Hou, Z. Shao, B. Yi. The effect of air stoichiometry change on the dynamic behavior of a proton exchange membrane fuel cell, J. Power Sources, 185, 2008, 302-310.

[28] H. Wang, X.Z. Yuan, H. Li. PEM Fuel Cell Diagnostic Tools, CRC Press, 2011, 578p, ISBN 9781439839195.